Chemical Engineering Journal 163 (2010) 413–421

Contents lists available at ScienceDirect

Chemical Engineering Journal

journal homepage: www.elsevier.com/locate/cej

Deactivation and coke combustion studies of nanocrystalline zeolite beta in catalytic cracking of used palm oil

Niken Taufiqurrahmi, Abdul Rahman Mohamed, Subhash Bhatia*

School of Chemical Engineering, Universiti Sains Malaysia, Engineering Campus, 14300 Nibong Tebal, Pulau Pinang, Malaysia

ARTICLE INFO

Article history:
Received 18 May 2010
Received in revised form 5 July 2010
Accepted 21 July 2010

Keywords:
Nanocrystalline zeolite beta
Catalytic cracking
Used palm oil
Deactivation
Coke combustion

ABSTRACT

Nanocrystalline zeolite beta was synthesized and its catalytic cracking activity for the production of biofuel from used palm oil was determined. The catalyst was characterized for its crystallinity, surface properties and morphology. The effect of reaction temperature on the catalytic cracking activity of nanocrystalline zeolite beta was also studied. The catalyst deactivation was monitored with the time on stream data by varying the palm oil to catalyst ratio of 6–14 at different temperatures. The deactivation data were analyzed using activity models and the deactivation parameters were obtained. The combustion behavior of the coked nanocrystalline zeolite beta derived at various coking temperature was studied by thermogravimetric analysis (TGA). The regeneration of the cracking catalyst was strongly correlated with the coke combustion kinetics. The coke combustion kinetics was studied and activation energy for coke combustion was determined.

1. Introduction

Zeolites are useful in many industrial processes because of their remarkable properties such as molecular sieving, acidity, high thermal stability, and shape selectivity. One of the most widely useful zeolite is zeolite beta. Zeolite beta has been used as an additive as well as catalyst in fluid catalytic cracking (FCC) of gas oil [1].

Currently, nanocrystalline zeolites received considerable attention due to their unique physico-chemical properties and added advantages. Reduction of their crystal size to nanometer could increase the reaction rate as a result of shorter diffusion paths of the reactant and product molecules inside the pores [2]. Landau et al. [3] reported that as the crystallite size of zeolite beta decreased from micrometer to nanometer, the rate constant and the effectiveness factor in hydrocracking of vacuum gas oil increased. Nanocrystalline zeolite beta exhibited a high degradation activity of HDPE, with high liquid product yield and high selectivity for C_7–C_{12} hydrocarbons [4].

The diminishing supply of fossil fuels and environmental pollution are the key factors leading to search for the alternative sources of energy besides fossil fuels. Different types of vegetable oils, edible and non-edible types are utilized in the production of biofuel. The choice of these raw materials depends mainly on its availability, cost and climate in each countries [5,6]. In general, the most abundant vegetable oil in a particular region is the most common feedstock. Palm oil is commonly used in the South-East Asia (mainly Malaysia and Indonesia) [6]. Oil palm is widely grown in Malaysia, in 2008 nearly 17.7 million tonnes of palm oil produced on 4.5 million hectares of land, and was the second largest producer of palm oil after Indonesia [7]. The high cost of the raw material has been one of the main drawback for the growth of biorefinery for production of fuels and chemicals from renewable resources. With the highest yield per hectare, palm oil is currently the world's cheapest and high volume edible oil that is being consumed makes it suitable choice of feedstock for the biofuel production [5].

However, the direct conversion of edible palm oil to fuel may not be economically feasible even though the results showed its potential of obtaining liquid hydrocarbons. Continuous and large-scale production of biofuel from edible oil without appropriate planning may cause negative impact on the food supply chain leading to economic problem [5]. A possible solution to overcome this problem is to utilize waste used edible oil or non-edible oil.

One of important criteria to determine the suitability of oil as a raw material for the production of biofuel, is the composition of the feedstock. The composition of oil subsequently determines the properties of the biofuel obtained. Generally, the physical and chemical properties of used palm oil (UPO) are almost similar to refined palm oil and may differ in the composition from source to source. Refined palm oil contained equal amount of saturated and unsaturated fatty acids. During cooking process, the palmitic and oleic acids concentration decreased in UPO. The drop in the concentration of fatty acids is compensated by the increase in the concentration of others types of fatty acids (palmitoleic acid, stearic acid, linoleic acid), respectively, beside the presence of water. The

* Corresponding author. Tel.: +60 4 5937788x6409; fax: +60 4 5941013.
E-mail address: chbhatia@eng.usm.my (S. Bhatia).

1385-8947/$ – see front matter © 2010 Elsevier B.V. All rights reserved.
doi:10.1016/j.cej.2010.07.049

Nomenclature

φ	activity of catalyst
Σs^2	sum of error squares
C_{c_0}	initial concentration of coke
C_c	instantaneous concentration of coke
E_a	activation energy (kJ/gmol)
k	rate constant
n_d	order of catalyst deactivation constant
k_d	rate of catalyst deactivation constant
m,n	reaction orders
P_{O_2}	partial pressure of oxygen (Pa)
R	universal gas constant, 8.31447 J/K gmol
R_c	the coke combustion rate (min^{-1})
R^2	regression coefficient
t	reaction time, min
T	experimental temperature

water content in UPO is relatively high as compared to the fresh edible oil as a result of frying process. During the frying process, palm oil is subjected to high temperatures in the presence of air and light at temperatures of 150–190 °C for a relatively long period of time. This results in the formation of a high number of new compounds through oxidation, hydrolysis, and polymerization reaction [8]. Some common physical changes were observed in used vegetable oil such as increase in viscosity and specific heat, higher tendency of fat formation, change in surface tension and color [5]. The extent of degradation of oil during frying process depends on the exposure temperature and time, frying oil, antioxidants and type of fryer. Hydrolysis increases the amount of free fatty acids, oxidation produces hydroperoxides and then low molecular volatile such as short chain alkanes, and dimers and polymers are also produced by radicals and Diels-Alder reaction [8]. Although UPO has less unsaturated fatty acids as compared to refined palm oil due to degradation after frying, the characteristic of the biogasoline produced from UPO is similar to biogasoline produced from palm oil in microreactor as reported in our earlier work [9]. The OLP, coke and gasoline fraction yields from UPO were still comparable with refined palm oil even though its gaseous products were higher. These findings show that there was not much difference between UPO and palm oil in terms of desired products distribution (OLP and gasoline fraction yields).

The production of biofuel with the choice of used palm oil as feedstock offers economic advantages over fresh palm oil. By converting used palm oil into fuel, it gives benefit to the environment by cleaning up the waste and converting them into value added chemical products and also without competing with the edible oil market as well as could be the feasible solution for overcoming the high cost of the raw material for biofuel production [5].

The catalytic cracking of vegetable oil process depends on the reaction operating conditions as well as the choice of catalyst [1]. The properties of catalysts are governed by acidity, pore shape and size [10]. Various types of zeolite catalysts are reported in the catalytic cracking for liquid fuel production from vegetable oil, palm oil, used palm oil and palm oil-based fatty acid mixtures (FAM) [9–15]. The catalytic cracking activity of commercial microcrystalline zeolite beta was investigated for the production of biofuel from waste used palm oil in our previous work [15]. Since large pore zeolites accommodate reactions of polynuclear aromatics or other bulky molecules, therefore zeolite beta (12-rings zeolite) could be a better option due to its higher accessibility. The shape selective characteristic of zeolite beta promoted the production of branched alkanes, alkenes and aromatics with high octane number [15]. However, due to its pore structure it was found that more coke was deposited on zeolite Beta in the cracking of both FAM and UPO [11].

One of the barriers in cracking reactions involving oil fraction is the solid acid cracking catalyst deactivation by the blockage of pores and active site coverage due to coke formation, depending on the catalyst age [16]. The deactivation could be expressed in terms of process time or the deactivating agent, i.e. coke on the catalyst, without explicit link to the operating conditions. The catalyst decay phenomenon could be quantified using empirical functions of the time on stream [17]. Serrano et al. [18] studied the deactivation and regeneration of nanocrystalline zeolite HZSM-5 for the cracking of polyethylene. Deactivated catalyst is usually regenerated before it can be reused. Catalyst regeneration is generally achieved by gradual heating under an oxidizing atmosphere. Therefore, the combustions kinetics of coke deposited on the deactivated catalyst provides useful information that helps in regeneration of catalyst.

There are number of studies reported on the kinetic models of coke combustion of different zeolites with various reactions using different methods [19–21]. In general, thermogravimetric analysis (TGA) has gained great acceptance [22]. A thermogravimetric method is proposed for observing different types of coke at different combustion temperatures and the kinetic parameters of catalyst regeneration can be obtained. TGA was also applied to examine the oxidative behavior of coke samples derived at various coking temperatures.

The understanding of catalyst deactivation and coke combustion is of great importance and has strong correlation. Thus, this allows the development of improved catalyst more resistant in deactivation and performs better during cracking process. In the present study an integral study of nanocrystalline zeolite beta as cracking catalyst for the production of biofuel from used palm oil is reported. The catalyst synthesis, characterization, catalytic activity in cracking of used palm oil, the effect of time on stream (TOS) on catalyst deactivation and coke combustion kinetics for regeneration of the catalyst are presented and discussed.

2. Experimental

2.1. Catalyst synthesis

Nanocrystalline zeolite beta was synthesized following the method reported by Modhera et al. [23]. NaOH pellets (0.2693 g) were diluted with an aqueous solution of 5.49 g TEAOH (35%, Sigma–Aldrich); 3.27 g Ludox AS-40 Colloidal Silica (40%, Sigma–Aldrich) was added to the mixture with vigorous stirring for 30 min to form a clear gel. An aqueous solution containing 0.2745 g aluminum sulphate ($Al_2(SO_4)_3$, Merck) was added to the mixture. The solution thus obtained was aged for 24 h under stirring at room temperature. The precursor gel had the molar composition as: $1SiO_2$:$0.2745Al_2O_3$:6.29TEAOH:$0.154Na_2O$. A viscous gel was obtained after ethanol formed during hydrolysis was evaporated. Finally, the crystallization of zeolite was carried out in a Teflon lined stainless steel autoclave (Parr reactor model 4842). After being filled with the prepared gel, the autoclave was completely sealed and heated at 140 °C and crystallization time was 48 h under autogenous pressure with stirring. The solid product was separated and recovered by centrifuge, washed several times with deionized water, dried overnight at 110 °C and calcined in air at 550 °C for 9 h. The solid was dried overnight at 110 °C. The synthesized catalyst (Na-form) was converted to H-form by refluxing with 0.5 M NH_4NO_3 aqueous solutions with liquid:solid ratio of 20 at 353 K and continuous stirring overnight. The resultant product was consequently filtered and washed with deionized water. The sample was kept to dry at room temperature overnight and then calcined at 550 °C for 4 h.

Table 1
Composition of used palm oil.

Fatty acid	Used palm oil (UPO) (%)
Lauric acid (C12:0)	1.1
Myristic acid (C14:0)	3.21
Palmitic acid (C16:0)	21.47
Palmitoleic acid (C16:1)	7.56
Heptadecanoic acid (C17:0)	0.51
Stearic acid (C18:0)	13
Oleic acid (C18:1)	28.64
Linoleic acid (C18:2)	13.58
Linolenic acid (C18:3)	1.59
Arachidic acid (C20:0)	0.64
Eicosenoic acid (C20:1)	–
Eicosadienoic acid (C20:2)	0.29
Arachidonic acid (C20:4)	0.37
Behenic acid (C22:0)	–
Lignoceric acid (C24:0)	–
Others	8.04

2.2. Characterization

The synthesized nanocrystalline zeolite beta was characterized using different techniques. The powder XRD patterns of zeolites were obtained using XRD measurement on a Philips diffractometer with Cu target Kα-ray. The analysis was conducted at 2θ values of 3–30°. For SEM observations, the powder samples were carefully placed on a double-sided tape with the aluminum stub as the base. The samples were coated with a thin layer of platinum for electron reflection using Polaron SC 515 sputter coater and scanned at different magnification. The samples were observed at different magnifications using a Leica Cambridge S-360SEM. The SEM analysis was extended to obtain quantitative composition of elements on the surface by analyzing the microscopic image under energy dispersive X-ray instrument (EDAX, INC). EDX Quantification software (GENESIS X-ray microanalysis software) was used to calculate the Si/Al ratio of the zeolite obtained. The powder sample was suspended in 100% ethanol under ultrasonic treatment for 15 min for TEM analysis. The TEM images were recorded using a Philip CM12 transmission electron microscope operated at 80 kV. Nitrogen adsorption–desorption measurements were conducted at 77 K on a Micromeritics ASAP 2020. The sample was first degassed for 3 h under vacuum at 573 K prior to the adsorption measurements.

2.3. Cracking activity test

The catalytic cracking activity test was performed at atmospheric pressure with reaction temperature range of 400–500 °C using a fixed-bed micro-reactor described elsewhere [12,14]. The used palm oil as the feedstock was obtained from university campus restaurant. The used palm oil was filtered to remove the solid impurities and was put in oven for 3 h to remove moisture prior to cracking activity test. Used palm oil consisted mainly of 28% C18:1 and 21% C16:0 fatty glycerides as shown in Table 1. The composition of used palm oil was determined in terms of different types of fatty acids present and their concentration using PerkinElmer Clarus 600 GC MS equipped with Elite 30-5 column (60 m × 0.25 mm × 0.25 mm). About 1 g of catalyst was loaded over 0.2 g of quartz wool supported by a stainless steel mesh in the micro-reactor (185 mm × 10 mm ID) placed in the vertical tube furnace (Model No. MTF 10/25/130, Carbolite). Once there was no change in the conversion of used palm oil at the temperature 450 °C, the steady state was reached. The liquid product was collected in a glass liquid sampler, while the gaseous products were collected in a gas-sampling bulb once the steady state was achieved. The unconverted oil was separated from the liquid product by distillation in a micro-distillation unit (Büchi B850, GKR) at 200 °C for 30 min under vacuum (100 Pa) with the pitch as the residual oil. Water was determined by separating the water from OLP. The gaseous products were analyzed using HP Plot Q capillary column (divinyl benzene/styrene porous polymer, 30 m long × 0.53 mm ID × 40 μm film thickness) equipped with thermal conductivity detector (TCD). The organic liquid product (OLP) was analyzed using a capillary glass column (Petrocol DH 50.2, film thickness 0.5 μm, 50 m long × 0.2 mm ID) at a split ratio of 1:100, using a FID detector. The composition of OLP was defined according to the boiling range of petroleum products in three categories, i.e. gasoline fraction (60–120 °C), kerosene fraction (120–180 °C) and diesel fraction (180–200 °C). The boiling range of each fraction was determined by injecting commercial samples of gasoline, kerosene and diesel in the gas chromatograph. The spent catalyst was washed with acetone to determine the residual oil and dried in oven at 200 °C before it was regenerated. Then it was calcined in a furnace at 600 °C for 3 h. The difference in the weight before and after calcination is the weight of coke formed in catalyst.

2.4. Deactivation (time on stream) studies

In order to determine the deactivation rate of the catalysts, a deactivation model was proposed by assuming that the catalyst activity (φ) is dependent on the time on stream (TOS), t. The total weight of oil injected into the reactor was varied at one selected feed rate. Since the time on stream data could not be collected in one run, change of oil to catalyst ratio with a fixed feed rate made it possible by changing the total time of the experiment as reported in our previous work [14]. In the present study, WHSV = 2.5 h^{-1} was used. The weight of oil was varied from 6 to 14 g at a fixed catalyst loading of 1 g. The catalyst activity (φ) is defined as the ratio of the rate of reaction at time t to the rate of reaction over a fresh catalyst ($t = 0$). The catalyst activity (φ) is defined as follows [17]:

$$\varphi(t) = \frac{\text{rate of reaction at time } (t = t)}{\text{rate of reaction at time } (t = 0)} \quad (1)$$

The rate of palm oil cracking was obtained at different time on stream. The rate of deactivation is presented as:

$$\frac{d\varphi}{dt} = -k_d \varphi^{n_d} \quad (2)$$

where k_d = deactivation rate constant and n_d = order of catalyst deactivation. The value of n_d and k_d could be estimated using nonlinear regression analysis method based on Levenberg–Marquard's algorithm [24] based on the best model fitted experimental activity data.

2.5. Coke combustion studies

The thermogravimetric/differential thermogravimetric (TG/DTG) study was performed using a thermogravimetric analyzer (Mettler Toledo, TGA/DSC 1) as described the literature [21,22]. In nonisothermal oxidation runs, a weighted amount of coked catalyst was heated from room temperature to 900 °C (20 °C/min) in an air atmosphere. In isothermal oxidation conditions, deactivated coked catalyst was heated to the combustion temperature (500–650 °C) under a nitrogen flow of 100 mL/min at a rate of 50 °C/min. Secondly, the combustion process was carried out by switching from the nitrogen flow to oxidative flow (N_2 and O_2). The oxygen partial pressure was kept at 8.9 kPa. The flow rate of the feed stream was regulated so the total gas flow rate was 100 mL/min. The TG and DTG data were continuously recorded and presented as percentage of the initial sample weight loss. For an isothermal oxidation run, the reaction time was shifted by a constant amount to adjust for warmup and hold of 15 min for the

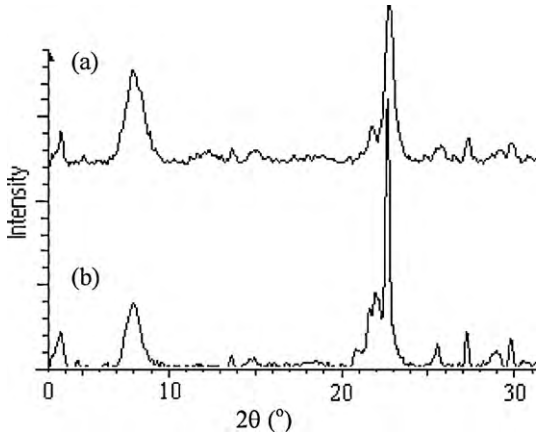

Fig. 1. X-ray diffraction of (a) nanocrystalline zeolite beta and (b) microcrystalline zeolite beta.

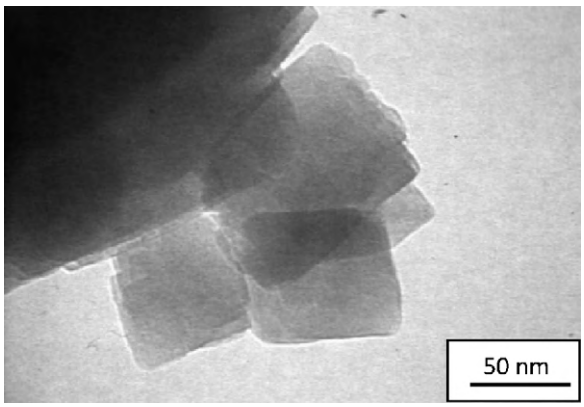

Fig. 3. TEM image of nanocrystalline zeolite beta.

removal of moisture. The initial time plot is at the first data point to achieve the final reaction temperature.

3. Results and discussion

3.1. Characterization

The XRD pattern of the nanocrystalline zeolite beta is shown in Fig. 1. The XRD pattern of commercial zeolite beta supplied by Sud Chemie (Si/Al = 15) is used as a reference (Fig. 1b). The XRD pattern of the sample was identical to that of the reference, the patterns comparison indicating the BEA structure of the nanocrystalline zeolite beta sample. There was a clear broadening of the reflections from the sample and decrease in the peak intensity, which was attributed to the presence of small crystals [25]. The crystallite size was estimated using the Scherrer equation [26]. With the corrected half width at half maximum (FWHM) of the most intense peak at $2\theta = 22.3^\circ$ for nanocrystalline beta [23]. The crystallite size for nanocrystalline beta was around 53 nm.

Representative SEM and TEM images of nanocrystalline zeolite beta are shown in Figs. 2 and 3, respectively. A small average crystal size of about 90 nm was observed in SEM images in fresh catalyst of nanocrystalline zeolite beta (Fig. 2a). Moreover, SEM images after regeneration are presented in Fig. 2b. Regenerated zeolite beta exhibited agglomerated ball-like isolated particles in the range of 100 nm. Fig. 3 shows the TEM images of nanocrystalline zeolite beta depicting its morphology.

The projected particle shapes in the TEM images tend to be close to square, which were consistent with nanocrystalline zeolite beta reported in the literature that the crystals transfer from the spherical crystal for microcrystalline zeolite and the squares crystals for 30 nm crystals [2]. A small crystal size of about 50 nm and its porosity was observed for nanocrystalline zeolite beta (Fig. 3) the crystal size distribution was uniform and spherical morphology was observed in SEM as well as TEM micrographs.

The specific surface area measured by the BET method, and *t*-plot method are used for the determination of external surface area, micropore surface area, and micropore volume, respectively. Surface properties of fresh, deactivated, and regenerated nanocrystalline zeolite beta are presented in Table 2. The large external surface area of the fresh catalyst of nanocrystalline zeolite beta (55% of the total surface area) shows that synthesized catalyst nanocrystalline zeolites beta possess small crystallites. The micropore volume of nanocrystalline zeolite beta was 0.148 cm^3/g. With the decrease in the crystal size, the micropore volume decreased as well [27].

In order to understand the coke deposition on the catalyst, deactivated catalyst nitrogen adsorption–desorption data was obtained. BET surface area for deactivated catalyst was 7 m^2/g, this surface area was contributed by external surface area, while micropore area reaches 0 m^2/g. The micropores were blocked with coke for the deactivated catalyst sample since no microporosity was detected from the nitrogen adsorption–desorption analysis. It is probable that the severe coking of the catalyst started from internal pore mouth plugging. These results were in a good agreement with previous report that the BET surface area of deactivated catalyst dropped to almost zero especially for catalyst with low Si/Al ratio [12]. After regeneration the surface area of nanocrystalline zeolite beta as well as micropore volume was slightly decreased from fresh catalyst, showing small impurities or coke still clog in pore of catalyst.

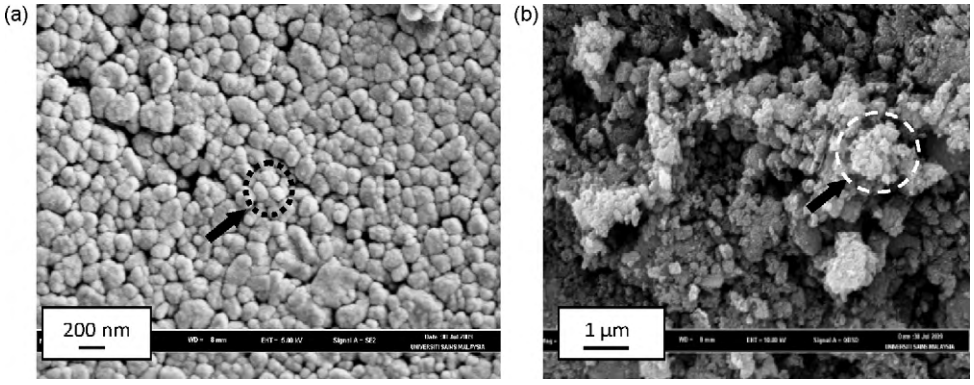

Fig. 2. SEM images of nanocrystalline zeolite beta (a) fresh catalyst and (b) used catalyst.

Table 2
Surface properties of nanocrystalline beta.

Sample	Surface Properties				
	S_{BET} (m^2/g)	External surface area (m^2/g)	Micropore area (m^2/g)	Micropore volume (cm^3/g)	Si/Al ratio[a]
Fresh catalyst	525	290	235	0.148	15
Deactivated catalyst	7	7	0	0.035	–
Regenerated catalyst	456	238	218	0.105	–

[a] From EDX analysis.

Fig. 4 shows the nitrogen adsorption isotherms of nanocrystalline zeolite beta. At low relative pressure ($P/Po = 0$) a steep increase in the amount of N_2 adsorption was exhibited, which corresponds to the filling of micropore with N_2, followed by nearly horizontal adsorption and desorption branches, a second uptake for high relative pressure with a hysterysis loop was observed around $P/Po = 0.9$, indicative of the intercrystalline textural mesoporosity. It can be seen that nanocrystalline zeolite sample has both micro-mesoporous features [27,28]. While deactivated catalyst reach 0 of adsorbed nitrogen, however after regeneration, nanocrystalline zeolite beta isotherm plot showed slightly different plot with fresh catalyst.

3.2. Catalytic cracking activity studies

The catalytic activity of nanocrystalline beta was determined from used palm oil (UPO) cracking. The cracking products were mainly organic liquid product (OLP), gaseous product, water and coke. The conversion of palm oil, yield and selectivity of product are defined as:

$$\text{Conversion (wt\%)} = \frac{[\text{Gas (g)} + \text{OLP (g)} + \text{Water (g)} + \text{Coke (g)}]}{\text{Used Palm Oil Feed (g)}} \times 100\% \quad (3)$$

$$\text{Yield (wt\%)} = \frac{\text{Desired Product (g)}}{\text{Used Palm Oil Fed (g)}} \times 100\% \quad (4)$$

$$\text{Selectivity (wt\%)} = \frac{\text{Desired Product (g)}}{\text{Used Palm Oil Converted (g)}} \times 100\% \quad (5)$$

Table 3 presents the conversion, yield of organic liquid product (OLP) and yield of coke over different reaction temperatures studied. The conversion and yield of gaseous products increased with the reaction temperature, achieving its highest value at highest temperature. The OLP slightly decreased at high temperature indicating that amount of OLP fraction was converted to gas. Similar trends were reported in the literature that the conversion of feed increased with temperature [10,12]. This was possibly due to the secondary cracking reaction, which was not active at lower reaction temperature.

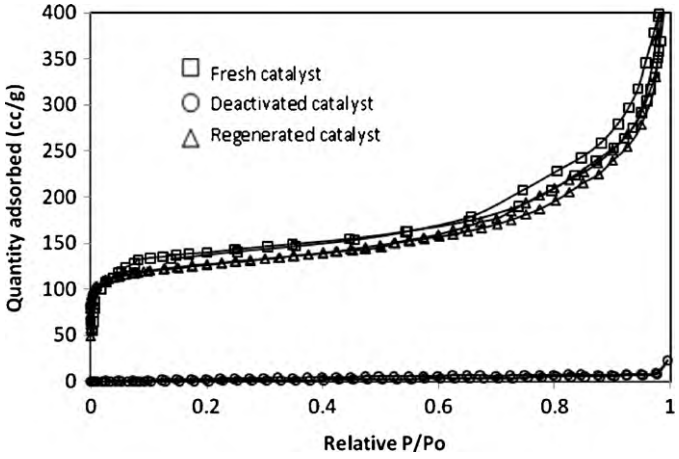

Fig. 4. Nitrogen isotherm of nanocrystalline zeolite beta.

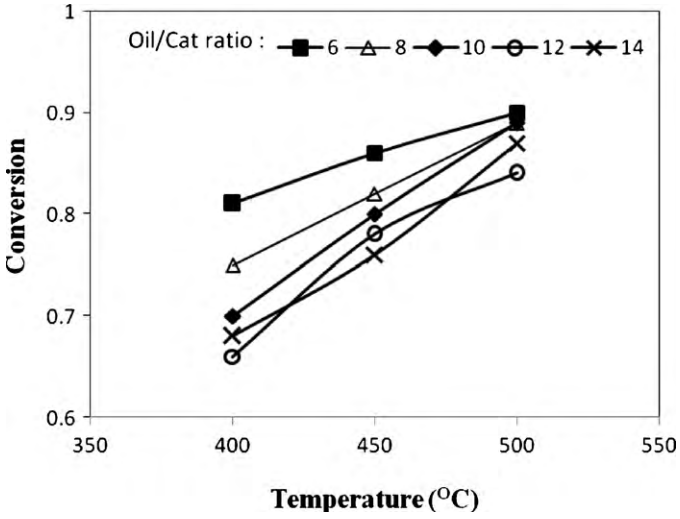

Fig. 5. Conversion of used palm oil over nanocrystalline zeolite beta at different cracking temperatures and oil/cat ratio (6–14).

Based on the used palm oil feed, the gasoline yield was between 35 and 40 wt%. The highest gasoline fraction value of 40 wt% was achieved at 450 °C. Compare to another acid cracking zeolite catalyst (ZSM-5), H-Beta exhibited relatively higher selectivity for kerosene fraction rather than gasoline fraction [15]. This phenomenon was due to low cracking rate of saturated fatty acids present in UPO and acidity of the zeolite Beta did not control the product selectivity due to accessibility limitation of the reactant [15].

Fig. 5 shows that at the same temperature, conversion changed with the variation in oil/catalyst ratio. The conversion of used palm

Table 3
Catalytic cracking of used palm oil over nanocrystalline zeolite beta with oil/catalyst ratio = 6.

Temperature (°C)	400	450	500
Conversion (wt%)	81	86	90
Product distribution (wt%)			
Gas	5	8	14
OLP	68	70	67
Water	4	6	7
Coke	4	2	2
Yield of OLP (wt%)			
Gasoline fraction	35	40	37
Kerosene fraction	21	23	22
Diesel fraction	10	7	8
Gas (wt%)			
Methane	2.9	0.6	1
Ethylene and ethane	9.4	2.6	5
Propylene and propane	16	8	9.5

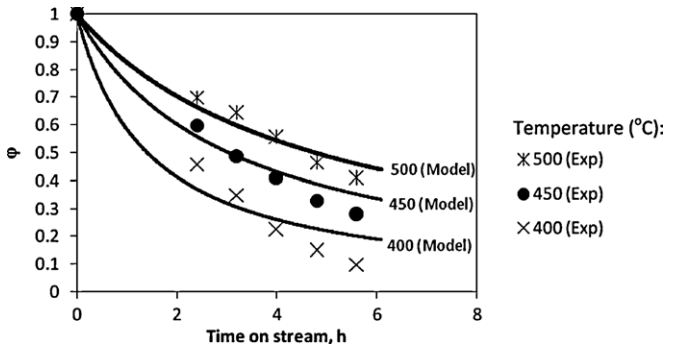

Fig. 6. Experimental and predicted activity data of used palm oil cracking over different cracking temperatures against time on stream.

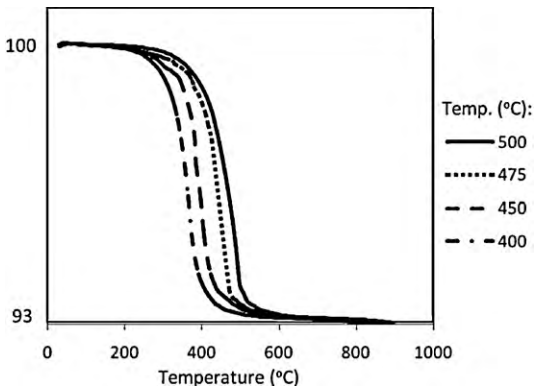

Fig. 7. Thermogravimetric curves of coked nanocrystalline zeolite beta derived at different cracking temperature with nonisothermal oxidation.

oil decreased with increasing oil to catalyst ratio due to the coke formation and its deposition on the catalyst surface and the pore blockage of micropores in the intra-wall. However, with an increase in temperature, the nanocrystalline zeolite beta presented its relatively stable activity at same temperature. These results show that at high temperature nanocrystalline zeolite beta deactivated slower. However, high conversion of used palm oil may not result in higher yield of organic liquid product. At high temperature, the yield of organic liquid product as well as the gasoline fraction dropped at the expense of gaseous product yield.

The deactivation model was developed by assuming that catalyst activity (φ) is dependent on the time on stream (h) (Eq. (1)). Fig. 6 shows time on stream data as well as activity model representing the cracking of UPO over nanocrystalline zeolite beta at different reaction temperatures. From the experimantal data, it can be observed that the catalytic activity of catalyst at all temperature dropped with time on stream due to the coke formation and its deposition on the catalyst. The stability of the catalyst structure also had significant effect on its activity since the catalyst samples were exposed to high temperature for long reaction time. The high coking was not only due to low silica–alumina ratio but also could be due to the geometrical freedom which enabled the formation of large polynuclear hydrocarbon. Zeolite beta possesses a three-dimensional pore system with straight channels of 0.73 nm × 0.65 nm and tortuous channels of 0.55 nm × 0.55 nm with a 1.0 nm channel intersections. These channel intersections probably allowed the trapping of coke precursor and resulted in the formation of bulky carbonaceous compounds.

Table 4 presents the value of deactivation rate constant, k_d, reaction order, n_d, calculated from best fitted model using nonlinear regression analysis method based on Levenberg–Marquard's algorithm (Eq. (2)). Fig. 6 also compares the predicted activity (model) obtained from the estimated values of n_d and k_d, with the experimental data. The experimental activity data of all model distributed close to the chosen model line data. The deactivation rate constant for nanocrystalline zeolite beta was different at different temperature used. However, it can be observed that at 500 °C nanocrystalline zeolite beta catalyst deactivated with lower deactivation rate constant of 0.3091 compare to lower temperature at 400 °C with deactivation rate constant of 0.3813. The higher value of deactivation rate constant at low temperature was due to its higher coke formation.

Table 4
Deactivation constant (k_d) and deactivation order (n_d) at different cracking temperatures calculated from the best fitted model.

Temperature (°C)	Model	n_d	k_d (h^{-1})	R^2	SSE
500	$\varphi = 1/(1 + k_d t)$	2	0.3091	0.91	3.6E−2
450	$\varphi = 1/(1 + k_d t)$	2	0.3277	0.94	1.4E−2
400	$\varphi = 1/(1 = k_d t)$	2	0.3813	0.92	7.2E−2

The R^2 for all temperature was more than 0.9 indicates that the hyperbolic model was quite reliable in predicting the deactivation kinetics of nanocrystalline zeolite beta (Fig. 6). It is reported in the literature that the cracking of gas oil followed the exponential law and also depends over time on stream operation [24]. However this assumption was not true in the present study of used palm oil cracking. The cracking mechanism in used palm oil differs from gas oil cracking because of the presence of different types of fatty acid glycerides. The gas oil is relatively heavier than used palm oil and also contains sulfur and heavy metals such as vanadium.

The Arrhenius law was applied to calculate the dependency of the deactivation rate constant (k_d) with temperature by plotting $\ln k_d$ against reciprocal of temperature. The value of deactivation energy was calculated to be −33.49 kJ/mol from Arrhenius law.

3.3. Coke combustion kinetics

3.3.1. Nonisothermal oxidation

Nonisothermal oxidation was carried on coked catalyst samples obtained from used palm oil catalytic cracking at different cracking temperatures as shown in Fig. 7. These curves indicate that the coke derived at 400 °C started the oxidation reaction at a lower temperature than the remaining coke samples. However, the different temperature among these samples is obvious, the coke produced at cracking temperature 400 °C start undergoing combustion at temperature around 380 °C whereas coke produced at cracking temperature 500 °C start combustion at 500 °C and the other samples remaining started combustion in between temperatures. It is shown that the start burned depends on the cracking temperature employed.

When the coking temperature increased, the temperature corresponding to the maximum oxidation rate also increased. Other results supporting this type of behavior were also reported by Ren et al. [22], the atomic H/C ratio decreased with the increasing pyrolysis temperature. This behavior can also be explained by the high volatility of coke precursors with increasing reaction temperature and their removal into gas phase, while at low temperatures the condensation of coke components was higher [29]. Moreover, it can be observed that the coke formed at high temperatures may be a high molecular weight substance having a very condensed structure, while the coke derived at low temperatures might have a less condensed structure.

3.3.2. Isothermal oxidation

3.3.2.1. TG-DTG characterization of the coked catalysts. The combustion temperature and the types of coke are needed to investigate the

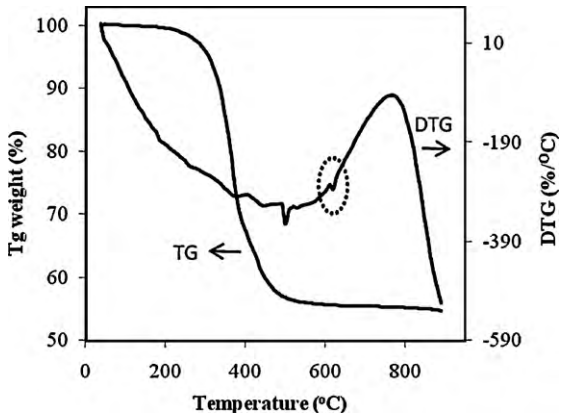

Fig. 8. TG/DTG curves of coked nanocrystalline beta on the basis of ramped temperature experiments.

kinetics of combustion of coked catalysts. On the basis of ramped temperature experiments, the TG-DTG curves of the coked catalysts were obtained as shown in Fig. 8. This sample was dried before experiment was conducted in TGA; therefore there was no peak below 100 °C which corresponds to adsorbed water. Two distinguishable negative peaks at about 450 and 620 °C were found as shown in Fig. 8. These two peaks indicate two types of coke on the catalyst derived from catalytic cracking which was in agreement with reported results [21]. The result indicates that one type of coke namely, the light coke can be removed below 550 °C. The peak at 610 °C in Fig. 9 is assigned to the heavy coke, which can only be removed at temperatures above 585 °C.

The amount of coke decreased as the coking temperature increased (Table 3). The coking at high temperatures was lower than that at low temperatures because of the lower condensation of coke components at high temperatures. For example, at oil/catalyst ratio = 6 and temperature 500 °C and 400 °C, coke content was 2 and 4 wt%, respectively. Less coke at high temperature results in high conversion.

3.3.2.2. One-coke oxidation reaction model. In the literature, it has been generally assumed that coke combustion is a one-pseudocomponent oxidation reaction [22]. The coke combustion

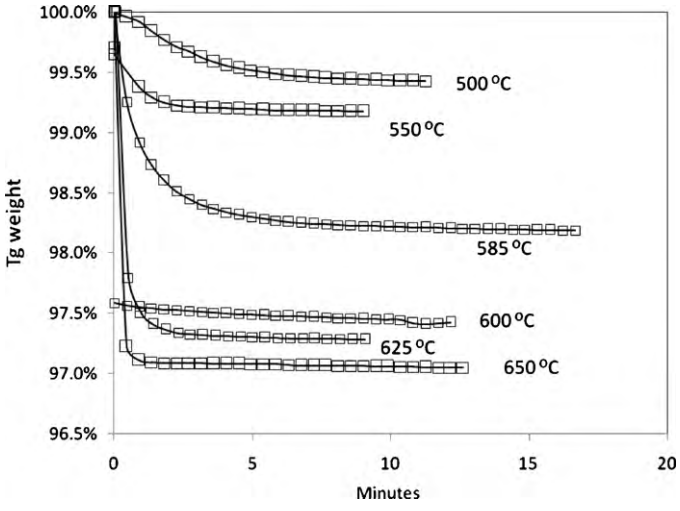

Fig. 9. Weight fraction of coked nanocrystalline zeolite beta (derived at 400 °C) at different temperatures under the same oxygen partial pressure of 8.9 kPa.

Table 5
Results of the reaction order of coked nanocrystalline zeolite beta (derived at 400 °C) at various combustion temperatures, P = 8.9 kPa.

	Temperature (°C)					
	500	550	585	600	625	650
n_2	1.09	1.08	1.08	1.07	1.05	1.03
$k_1 P^m$ O_2	0.06	0.125	0.335	0.549	0.687	0.925

rate, R_c can be described in terms of instantaneous concentration of coke (C_c), rate constant (k), partial pressure of oxygen (P_{O_2}), reaction orders (m,n) and reaction time (t). The coke combustion rate, R_c, can be presented as [13,18,19]:

$$R_c = \frac{-dC_c}{dt} = kP_{O_2}{}^m C_c^n \tag{6}$$

The reaction rate constant k is a function of temperature (T) can be expressed as:

$$k = A_r \exp\left(\frac{-E_a}{RT}\right) \tag{7}$$

If, during isothermal oxidation, the change in the oxygen partial pressure is small and n = 1, Eq. (6) can be expressed as:

$$\frac{-dC_c}{dt} = k_1 C_c \tag{8}$$

$$\ln\left(\frac{C_c}{C_c^0}\right) = -k_1 t \tag{9}$$

where k_1 = pseudofirst order rate constant.

If the partial pressure of oxygen (P_{O_2}) is fixed, the non-linear regression of the DT-DTG curves at different temperatures can determine the parameter of the reaction order n and activation energy, E_a from Eq. (10) as given below:

$$\ln\left[\frac{-dC_c}{C_c^n\, dt}\right] = \ln kP_{O_2}^m = \ln A_0 + \left(\frac{-E}{R}\right)\left(\frac{1}{T}\right) + m \ln P_{O_2} \tag{10}$$

3.3.3. Determination of the reaction order n

For an isothermal oxidation run, the reaction time was shifted by a constant amount to adjust for warmup. Here, the first data point to achieve the final reaction temperature was assigned as the initial time. Hence the reaction time was defined as the difference between the initial reading and the final one.

TG curves of coked nanocrystalline zeolite beta (cracking temperature: 400 °C) at different temperatures under the oxygen partial pressure of 8.9 kPa are shown in Fig. 9. The combustion rate increased with the reaction temperature. It appears that, the light coke is reactive below 550 °C, while in contrast, the heavy coke is inactive until the temperature is higher than 585 °C. Non-linear regression was performed for determining the reaction order n by using a trial-and-error method. In the present study, the numerical simulation was carried out by using MATLAB software [21].

The regression results are presented in Table 5 and Fig. 10. The light coke was burnt out prior to the combustion of the heavy coke. This result shows the much lower activation energy of the light coke combustion is needed. Furthermore, the reaction order n determined by non-linear regression is nearly 1, which indicates that the reaction rate of light coke is a little more sensitive to the content of coke.

As reported in the literature that, for coke combustion, if, during isothermal oxidation the change in the oxygen partial pressure is small or partial pressure of oxygen is fixed, the value of n (the reaction order) is one [21,22]. Moreover, Eqs. (6) and (7) can be expressed as Eq. (10) to create an Arrhenius plot by linear regression through a set of isothermal oxidation runs with C_{c_0} is the initial concentration of coke. In TGA experiments, C_c/C_{c_0} can be taken as

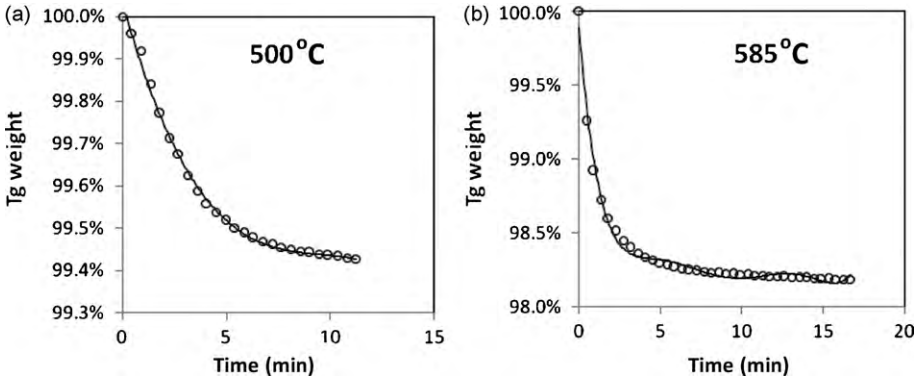

Fig. 10. Non-linear regression of experimental data during combustion of coked nanocrystalline zeolite beta (derived at 400 °C) at different temperatures: (a) 500 °C and (b) 585 °C.

Table 6
Activation energy from isothermal combustion of coked nanocrystalline zeolite beta at different cracking temperature.

Coking temperature (°C)	E_a (kJ/mol)
400	118.45
425	155.70
450	157.37
475	157.79
500	157.79

the instantaneous weight of coke left on the pan, in units of weight percent. The weight versus time of material left on the TGA pan was numerically calculated from Eqs. (7) and (10). The Arrhenius plot method was applied to determine the kinetic parameters for the one-coke model from isothermal oxidation runs for the coke derived at cracking temperature 400–500 °C (Table 6). It can be observed that the higher coking temperature caused the coke's oxidation activation energy to be higher [19,22].

The activation energy (E_1) of the light coke was 118 kJ/mol, much lower than that of the heavy coke, which was about 157 kJ/mol. This result proves that the heavy coke was more resistant to combustion than the light coke. The activation energy of 157 kJ/mol, was in agreement with the value computed in reported study for the laboratory coked zeolite [19]. It can be observed that there are three zone of the activation energy for coke derived from different cracking temperature, namely: less than 400 °C, 400–450 °C, and higher than 450 °C which in this zone the activation energy was quite stable. Coke formation has been regarded as a complex reaction strongly affected by the catalyst structure, and the character of the coke varied with the kind of reactants and the reaction conditions.

4. Conclusions

Nanocrystalline beta is a promising catalyst in cracking of used palm oil for the biofuel production. The catalyst showed appreciable activity with high palm oil conversion and gasoline yield of 35–40 wt%. However, with geometry of zeolite beta, produced high coke content, which contributed to deactivation of the catalyst. With increase in reaction temperature, the deactivation rate could decrease slightly. This was due to lower coke amount produced as the coking temperature increased. However when the coking temperature increased, coke formed may be of high molecular weight substance type, having a very condensed structure. Moreover, heavy coke was more resistant to combustion than the light coke, as found from the higher activation energy of the heavy coke combustion.

Acknowledgements

The authors gratefully acknowledge the financial support provided by the Ministry of Science, Technology and Innovation (MOSTI), Malaysia under e-Science fund (Project: 03-01-05-SF0221), Research University Grant (grant number: 811043) Universiti Sains Malaysia, Penang and also Universiti Sains Malaysia Post Graduate Research Scheme (Project: 1001/PJKIMIA/8032011) to carry out this study.

References

[1] S. Bhatia, Zeolite Catalysis: Principles and Applications, CRC Press, Florida, 1990.
[2] L. Ding, Y. Zheng, Nanocrystalline zeolite beta: the effect of template agent on crystal size, Mater. Res. Bull. 42 (2007) 584–590.
[3] M.V. Landau, L. Vradman, V. Valtchev, J. Lezervant, E. Liubich, M. Talianker, Hydrocracking of heavy vacuum gas oil with a Pt/H-beta–Al_2O_3 catalyst: effect of zeolite crystal size in the nanoscale range, Ind. Eng. Chem. Res. 42 (2003) 2773–2782.
[4] Y.J. Lee, J.-H. Kim, S.H. Kim, S.B. Hong, G. Seo, Nanocrystalline H-beta zeolite: an efficient solid acid catalyst for the liquid-phase degradation of high-density polyethylene, Appl. Catal. B: Environ. 83 (2008) 160–167.
[5] M.M. Gui, K.T. Lee, S. Bhatia, Feasibility of edible oil vs. non-edible oil vs. waste edible oil as biodiesel feedstock, Energy 33 (2008) 1646–1653.
[6] B.K. Barnwal, M.P. Sharma, Prospects of biodiesel production from vegetable oils in India, Renew. Sust. Energy Rev. 9 (2005) 363–378.
[7] MPOB, Economic and statistic: MPOB 2010, see also: <http://www.mpob.gov.my/html/05_pi/gfx_bs/bs79_13a.jpg>.
[8] E. Choe, D.B. Min, Chemistry of deep-fat frying oils, J. Food Sci. 72 (2007) R77–R86.
[9] N.A. Ahmad Syah, Nanostructured materials as catalysts for the production of gasoline from used palm oil and crude palm oil: synthesis, characterization and activity studies. M.Sc. thesis, Universiti Sains Malaysia, Malaysia (2007).
[10] P. Tamunaidu, S. Bhatia, Catalytic cracking of palm oil for the production of biofuels: optimization studies, Biores. Technol. 98 (2007) 3593–3601.
[11] Y.-S. Ooi, Composite micro-mesoporous materials for the production of liquid fuels from catalytic cracking of fatty acids mixture and used palm oil, Ph.D. thesis, Universiti Sains Malaysia, Malaysia (2004).
[12] Y.-S. Ooi, S. Bhatia, Aluminum-containing SBA-15 as cracking catalyst for the production of biofuel from waste used palm oil, Micropor. Mesopor. Mater. 102 (2007) 310–317.
[13] R.K. Sharma, N.N. Bakhshi, Upgrading of tall oils to fuels and chemicals over HZSM-5 using various diluents, CJChE 69 (1991) 1082–1086.
[14] S. Bhatia, A.R. Mohamed, N.A.A. Syah, Composites as cracking catalysts in the production of biofuel from palm oil: deactivation studies, Chem. Eng. J. 155 (2009) 347–354.
[15] Y.-S. Ooi, R. Zakaria, A.R. Mohamed, S. Bhatia, Synthesis of composite material MCM-41/beta and its catalytic performance in waste palm oil cracking, Appl. Catal. A: Gen. 274 (2004) 15–23.
[16] V.J. Fernandes Jr., A.S. Araujo, Kinetic study of H–Y zeolite regeneration by thermogravimetry, Thermochim. Acta 255 (1995) 273–280.
[17] H.S. Fogler, Elements of Chemical Reaction Engineering, 3rd ed., Prentice Hall International, 2006.
[18] D.P. Serrano, J. Aguado, J.M. Rodriguez, A. Peral, Catalytic cracking of polyethylene over nanocrystalline HZSM-5: catalyst deactivation and regeneration study, J. Anal. Appl. Pyrol. 79 (2007) 456–464.
[19] V.D. Dimitriadis, A.A. Lappas, A. Lacovos, Vasalos, Kinetics of combustion of carbon in carbonaceous deposits on zeolite catalysts for fluid catalytic cracking units (FCCU). Comparison between Pt and non Pt-containing catalysts, Fuel 77 (1998) 1377–1383.

[20] G.J. Heynderickx, E.M. Schools, G.B. Marin, Coke combustion and gasification kinetics in ethane steam crackers, AIChe J. 51 (2005) 1415–1428.
[21] N. Zhu, Y.-Y. Liu, Y. Wang, F.-Q. Chen, X.-L. Zhan, Kinetic models for the coke combustion on deactivated ZSM-5/MOR derived from n-heptane cracking, Ind. Eng. Chem. Res. 49 (2010) 89–93.
[22] Y. Ren, N. Mahinpey, N. Freitag, Kinetic model for the combustion of coke derived at different coking temperatures, Energy Fuels 21 (2007) 82–93.
[23] B. Modhera, M. Chakraborty, P.A. Parikh, R.V. Jasra, Synthesis of nano-crystalline zeolite beta: effects of crystallization parameters, Cryst. Res. Technol. 44 (2009) 379–385.
[24] J. Ancheyta-Juarez, F. Lopez-Isunza, E. Aguilar-Rodriguez, 5-Lump kinetic model for gas oil catalytic cracking, Appl. Catal. A: Gen. 177 (1999) 227–235.
[25] M. Singh, K. Raviraj, N. Viswanadham, Effect of crystal size on physico-chemical properties of ZSM-5, Catal. Lett. 120 (2008) 288–293.
[26] B.D. Cullity, S.R. Stock, Elements of X-ray Diffraction, 3rd ed., Prentice Hall, New Jersey, 2001.
[27] G. Majano, A. Darwiche, S. Mintova, V. Valtchev, Seed-induced crystallization of nanosized Na-ZSM-5 crystals, Ind. Eng. Chem. Res. 48 (2009) 7084–7091.
[28] J. Parmentier, V. Valtchev, F. Gaslain, L. Tosheva, D.-B. Claire, J. Möller, J. Patarin, C. Vix-Guterl, Effect of the zeolite crystal size on the structure and properties of carbon replicas made by a nanocasting process, Carbon 47 (2009) 1066–1073.
[29] B. Wang, G. Manos, Deactivation studies during 1-pentene reactions over HUSY zeolite, Chem. Eng. J. 142 (2008) 217–223.